Destruction of Darkness: Optical Coherence Effects and Multi-Wave Mixing in RubidiumVapor

A.S. Zibrov[1,2,3], L. Hollberg[1], V.L. Velichansky[2,3], M.O. Scully[2,4], M.D. Lukin[5], H.G. Robinson[1], A.B. Matsko[2], A.V. Taichenachev[6], and V.I. Yudin[6]

[1] *NIST, 325 Broadway, Boulder, CO, USA, 80303,*
[2]*Texas A&M University, College Station TX, 77843and*
[3]*Lebedev Institute of Physics, Moscow, Russia*
[4]*Max-Planck-Institut für Quantenoptik, 85748 Garching, Germany*
5Harvard Smithsonian, Cambridge, MA 02138,
[6]*Novosibirsk State University,Novosibirsk, Russia*
hollberg@boulder.nist.gov, http//www.bldrdoc.gov/timefreq/ofm

Abstract. We describe several novel experimental effects resulting from optical coherences in multilevel atoms driven with coherent laser fields. Four configurations were explored using Rb vapor cells: lambda dark-line resonances, single beam double-lambda oscillations, and cascade two-photon transitions in co- and counter-propagating geometries. Experiments were performed with high spectral-resolution using low-power diode lasers sources and optically thick cells. Two of the most striking effects we observed are: (1) a self-oscillation that occurs at 3.0 GHz on the ^{85}Rb hyperfine frequency when a single laser field pumps the atoms, and (2) a coherent blue-beam emission that we observe in the co-propagating cascade two-photon case. These phenomena lead to complex lineshapes, and the effects sometimes dominate the well-known 3-level coherence effects. Additional higher-order mixing or cascaded interferences are apparent in all four experimental configurations. Many of these can be viewed as multi-wave mixing enhanced by optical coherences around closed-loop paths of atomic energy levels. The effects are particularly strong when four-photon closed-loop paths with resonant energy levels are possible, as in, the double-lambda system or as a four-wave mixing "box."

INTRODUCTION

Motivated by the desire to understand atomic coherence effects in multilevel atoms, we have been studying characteristic lineshapes in lambda and cascade 2-photon transitions with variations in experimental parameters. We continue to be surprised by the richness of phenomena that occur when even low-power laser beams interact with reasonably dense atomic vapors. Better knowledge and control of these systems should allow us to take advantage of the novel coherence effects (coherent population trapping (CPT), electromagnetic induced transparency (EIT),

CP551, *Atomic Physics 17*, edited by E. Arimondo, P. DeNatale, and M. Inguscio
2001 American Institute of Physics 1-56396-982-3

and gain without inversion, etc.) to develop advanced sensors and sources of radiation. Examples are: microwave frequency references, short-wavelength lasers, and media with high indices of refraction or tailored group velocities. Significant research efforts have been recently directed toward the study of these effects in similar systems, with interesting experimental results reported from the groups of Arimondo, Dunn, Ducloy, Hänsch, Harris, Hemmer, Lange, Wellegehausen, Wynands, and many others. Distinguishing aspects of the present work include the use of low-power cw laser sources, very high spectral resolution, and atomic vapors that are relatively dense. Optically thick atomic vapors offer potential advantages including long, effective interaction lengths, bigger signals and, sometimes, narrower linewidths. If we can achieve good transparency at high densities, then more atoms can contribute to the signal, and the spectral features could be narrowed due to exponential absorption through the cell. In addition, with long interaction lengths, dispersive and other nonlinear processes become important. These processes can significantly alter the character of the signal, sometimes interfering with, sometimes enhancing and often creating new structure within the lineshape.

This paper focuses on how these nonlinear interactions affect four different experimental configurations: the "Dark-Line" lambda resonance of Gozzini's group [1], a single-beam double-lambda oscillation, the cascade two-photon system with counter-propagating beams, and the cascade two-photon system with co-propagating beams. The underlying 3-level systems have been carefully studied over the past 20 years [2,3]. Our emphasis here is on laboratory results viewed from the experimentalist's perspective as opposed to detailed analysis of the systems. Obviously both theory and experiment are required to properly understand the results.

Perhaps the most interesting regime was when the laser field was strong (Rabi frequency large compared to the spontaneous decay rate of the atom) and the cells optically thick. This regime can give large signals with narrow linewidths, the result being improved signal-to-background and a high quality-factor, Q. All four experiments were performed with Rb vapor cells that could be heated, and with either one or two input fields from tunable diode lasers. The lasers were extended-cavity-diode-lasers (ECDL) with output powers from 10 to 35 mW, except in one case a semiconductor tapered-amplifier was used with >100 mW at 776 nm. The optical intensity applied to the atoms varied greatly, with Rabi frequencies, Ω_R, ranging from 0.01 to 10 times the spontaneous decay rate, Γ. In most cases $\Gamma < \Omega_R < \omega_D$ where ω_D is the Doppler width of the transitions involved. Cells with natural isotopic abundance were used at temperatures from room temperature up to 200 C (473 K), and lengths ranging from 3 to 10 cm, incorporating a variety of different kinds of cell windows.

DARK-LINE LAMBDA RESONANCES

The first case we consider is the "dark-line" resonance in the Λ-configuration with an optically thick cell and co-linearly propagating input beams. In some conditions, by increasing the optical thickness it is possible to retain high contrast while simultaneously narrowing the spectral linewidth. Narrower linewidths, paired with high contrast, result in larger signals and reduced background. This combination

might have advantages in some applications of dark-line resonances such as compact, low-power, microwave frequency references [4,5] or for magnetometers [6,7]. Early proponents of using optically thick cells to enhance nonlinear transparencies include: work by Svanberg and Schawlow [8], using the population effects of saturated absorption, and Harris et al. who has shown spectacular results in changing transparency over orders of magnitude using the coherence effects of EIT [9,10]. In our experiments we utilize optical coherences to obtain spectrally narrow linewidths with high-contrast, and study the details of the spectral lineshapes to gain a better understanding of the interactions.

Our first experimental system is quite simple: two ECDL lasers provide the input fields to the Rb cell. The lasers were tuned near the 795 nm D1 line, and one laser was phase-locked to the other with a variable frequency offset near the ground-state hyperfine splitting of 6.8 GHz. The signal we detected was the power in the beatnote (at 6.8 GHz) between the two lasers after they passed through the Rb cell. This method allowed us to probe the structure of the dark-line resonance with a high signal-to-noise ratio, and with synthesizer precision in the offset frequency. Figure 1 shows the structure of the "dark-line" that we observed as a function of frequency offset for different cell temperatures.

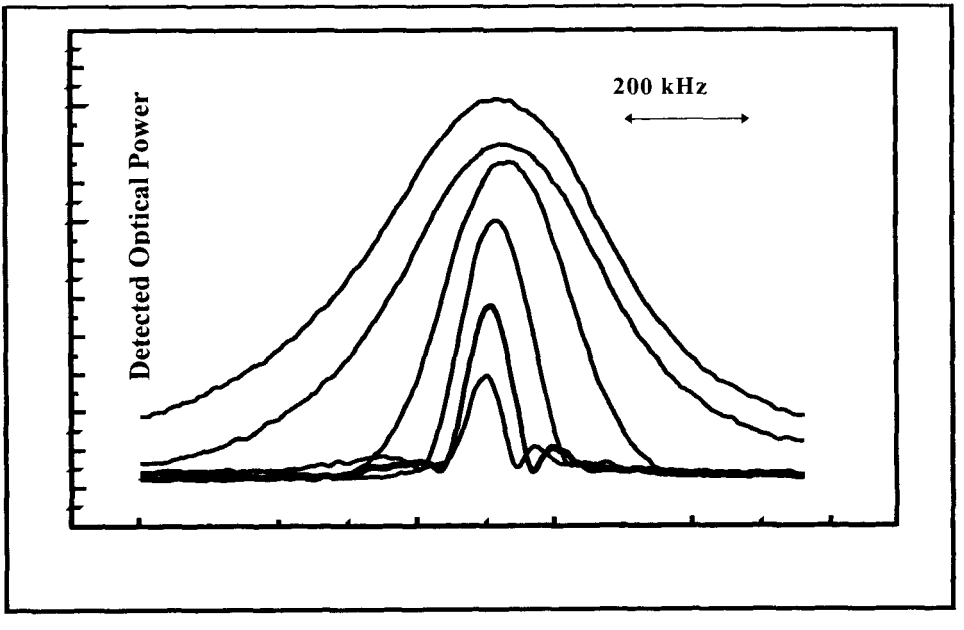

FIGURE 1. Power detected in the beatnote between the two phase-locked lasers transmitted through the Rb cell as a function of the microwave frequency offset between them. The six curves from largest to smallest correspond to the cell temperatures, 52, 57, 72, 80, 85 and 89 C. The lasers were tuned to the D1 transition at 795 nm, F=2 to F'=2, with their difference frequency centered on the ^{87}Rb hyperfine splitting of 6.8 GHz. As the cell is heated, the dark-line narrows due to exponential absorption in the wings of the resonance. The transparency (and detected signal shown here) decrease and additional interfering structure appears in the lineshape at the higher temperatures (lower curves). Laser powers were a 5.6 mW/ 3 mm dia. and 0.1 mW / 3 mm diameter, and the cell's length was 5 cm.

As the cell temperature increased the optical thickness increased and the linewidth of the "dark-line" resonance became narrower as desired and expected. With higher temperatures the transparency began to decrease and additional structure appeared in the lineshape, as seen in fig.1. As the optical depth reached the range of the two higher temperature curves, we saw the clear signature of interference effects on the lineshape. The transparency of the "dark-line" resonance seems to be destroyed by spectrally narrow dips that appear in the resonance. These features result from an additional field generated by the atoms via a double-lambda type interaction with the two input fields as diagrammed in fig. 2.

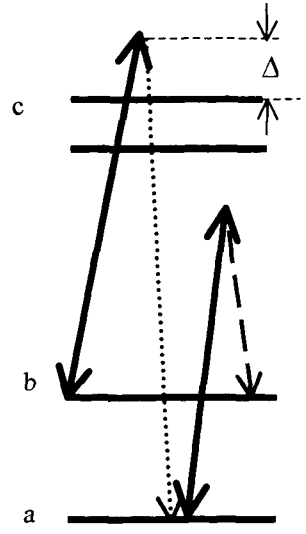

FIGURE 2. Simplified energy-level diagram of Rb showing the configuration of the input laser field(s) (indicated by the dark solid line and the dotted line) and the fields generated by the Rb atoms (dotted line plus dashed line) in the "double-lambda" interaction. The dotted line is the anti-Stokes component and the dashed line is the Stokes component.

This new field (the Stokes component in the example of fig. 2) also makes a beatnote with the strong drive-field; the beatnote is offset in frequency by the hyperfine splitting of the ground state. This additional beatnote has the same frequency offset relative to the drive (but opposite in sign) as the original beatnote generated by the dark-line resonance. Thus, the photo-currents from the two beatnotes interfered with each other in the detector, and appeared as an enhancement or a zero in the detected signal.

The effects of optical pumping and optical coherences around closed-loop double-lambda paths are critically important in understanding the details of the lineshape [11, 12]. Theoretical models including coherent-coupling between all the fields and atomic levels provide excellent agreement with the experimental lineshapes results [13].

Dark-Line Λ-Resonance With Optical Feedback

More dramatic effects become apparent in this lambda-CPT system if even a small amount of the transmitted beam travels backward through the atomic vapor. A counter-propagating beam (for example, reflection from the cell window) causes the system to "self-oscillate" at the ground state hyperfine splitting of 3.036 GHz. In this case, we observed that with a single laser-field incident on the Rb cell (tuned near the ^{85}Rb D2 line) the transmitted beam developed strong AM modulation at the frequency of the hyperfine splitting. The experimental apparatus is shown schematically in fig. 3.

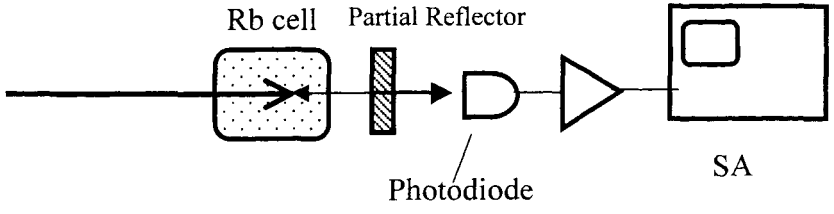

FIGURE 3. A single laser field from an ECDL is sent through a heated Rb cell, and part of the transmitted light (4 to 80 %) is reflected back through the cell by the partial reflector. A fast photodiode, amplifier and spectrum analyzer (SA) are used to display the microwave spectrum of the power fluctuations on the transmitted laser beam. Under conditions outlined in the text we observed a strong (60 dB signal to noise in 30 kHz bandwidth) and narrow (< 300 Hz) beatnote at the ground-state hyperfine splitting of ^{85}Rb, 3.036 GHz.

Thus, a 10 mW laser beam tuned near resonance shows large AM modulation sidebands that appear on the transmitted laser beam at the 3.036 GHz, ^{85}Rb hyperfine splitting (hfs). The AM sidebands have the same spectral characteristics as the input laser field, and produce a narrow linewidth beatnote with the carrier (<300 Hz FWHM at 3.036 GHz). We have observed as much as 4 % of the transmitted power contained in each of the frequency-shifted sidebands. A higher-order anti-Stokes sideband (up-shifted from the carrier by twice the ground state hyperfine splitting) was also observed under some conditions.

In contrast to our usual experience with a single laser field tuned near the D2 resonance in Rb, the atoms do not get pumped into a "dark state". In fact, the system refuses to go dark and becomes strongly interacting. The net effect is to scatter photons from the input laser field to new frequencies, shifted both up and down from the input laser frequency by the ground state hfs. With the reflected-light traveling backward through the cell the system remains in a bright-state even though there is complex hyperfine and Zeeman structure that allows many different possible dark-states. The transmitted light thus contains the input carrier-field, plus an upper and lower sideband. We studied the spectral properties of the transmitted light by making a beatnote with an independent laser, and also by analyzing the spectra with a Fabry-Perot cavity. A Fabry-Perot spectrum of the beam transmitted through the cell is shown in fig. 4.

At least for the range of experimental parameters accessible in our apparatus, the backward-going reflection of the transmitted light was critical to observe the strong

and narrow self-oscillation. For example, the oscillation did not appear if the input laser was first divided into two beams and sent through the cell in opposite directions. By using an independent, tunable, diode laser we determined that the oscillation could be initiated most easily by sending a laser backward through the cell that was tuned to the anti-Stokes frequency. In the single-laser geometry the beam transmitted through the cell will contain some anti-Stokes component, which, when reflected back into the cell can initiate the self-oscillation.

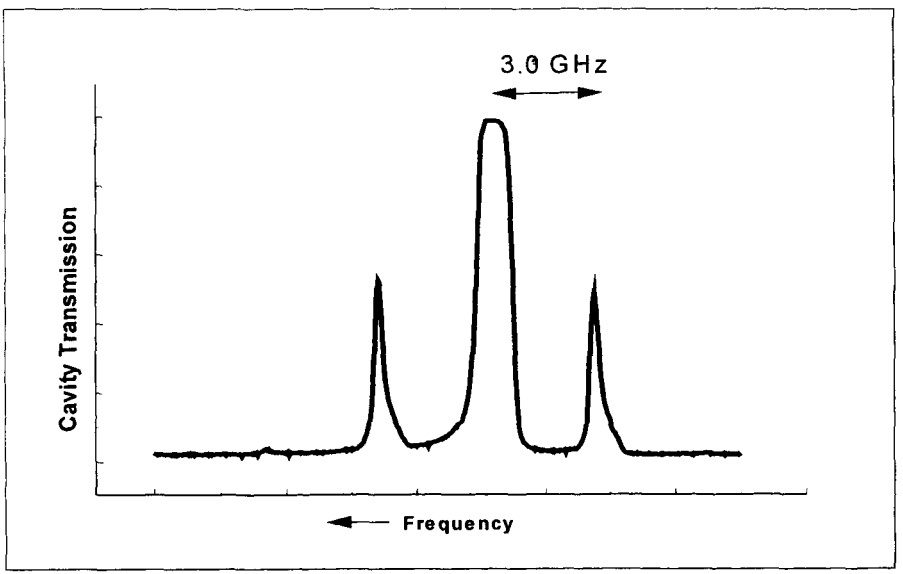

FIGURE 4. This trace shows a Fabry-Perot cavity spectrum of the light transmitted through the Rb cell in the configuration of fig. 3. and when the system is in self-oscillation at the hyperfine frequency. The oscillation is caused by the backward-going beam from the partial reflector. The smaller peaks on either side of the incident carrier were generated in the Rb vapor and correspond to the fields represented in fig. 2. by the dotted and dashed lines. The sidebands are separated from the input carrier by 3.036 GHz and each contains approximately 4 % of the power in the strong carrier, which is clipped at the top of the figure.

In the case of ^{85}Rb the oscillation only requires a single input laser field, while for ^{87}Rb some additional hyperfine re-pumping was required to see the corresponding oscillation at 6.8 GHz. Although these nonlinear oscillations and interferences are important in understanding the fundamental interaction of laser fields with alkali atoms, we have not yet found a way to use them to improve the performance of our compact microwave frequency references [4]. In fact, these interactions seem to be mostly detrimental; but this, in itself, means that it is critically important to understand the interactions and how they can affect the low intensity, low vapor-density CPT clocks that we are also studying [5]. Nonetheless, the effects may be quite useful in enhancing dispersion and altering the group velocity and index of refraction for other applications.

CASCADE 2-PHOTON COUNTER-PROPAGATING

The third experimental configuration that we studied was that of counter-propagating beams near the cascade 2-photon resonance (5S-5P-5D) in a Rb cell. The idea was to explore the potential for observing a high index-of-refraction, and/or the large changes in group-velocity associated with the coherences in near-resonance two-photon transitions when the atomic vapor is optically thick. Here we used even higher cell temperatures, a strong field on the upper part of the two-photon transition propagating in the forward direction, and a weak probe-field on the resonance line propagating in the backward direction. The probe penetrates only a short distance into the cell, but the coherent effects are detected on this beam in reflection from the cell window. Near resonance we see the well known "selective reflection" (SR) signals [14, 15]. These signals are also complicated by additional multi-wave mixing signals that appear under many conditions. Related effects have also been reported and studied in detail by Ducloy and collaborators. They have observed surprising non-phase-matched four-wave-mixing (4WM) signals in reflection from Cs vapor cells [16]. We detect additional unexplained structure in Rb as well, but we also find phase-matched 4WM in reflection from the cells. In the usual reflection geometry it is difficult to separate the effects of SR from those of multi-wave mixing. However, the SR signal can be unambiguously separated from the phase-matched 4WM signal using the experimental geometry outlined in fig. 5.

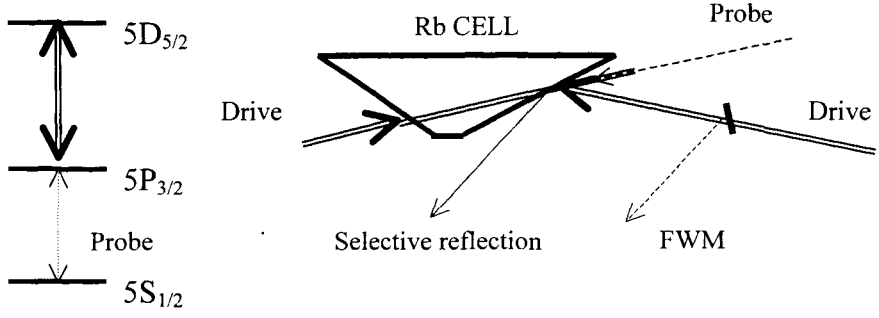

FIGURE 5. Experimental configuration used for separating the SR and 4WM signals. The two strong drive-fields (from a single amplified ECDL) are tuned to the 776 nm upper half of the two-photon cascade, and the weak probe laser is tuned to the 780 nm D2 line. The angle between the probe and the backward drive is ~ 3^0, which has been exaggerated in the figure for clarity.

We find regimes where the multi-wave mixing is much larger and much narrower than the SR signals that are induced by index-of-refraction effects. On resonance, with a heated cell, the probe-field penetrates only a very short distance into the atomic vapor; yet it was possible to have gain (as much as 130% in reflection) in the 4WM reflection signal. Examples of the signals that we observed using the reflection geometry above (fig. 5.) are shown in fig. 6. The selective-reflection signals, SR, are Doppler-free and have widths of about 60 MHz, while the 4WM resonances are larger

and narrower (FWHM ~2 MHz) and are sensitive to the relative phase of the two drives-fields and the probe-laser field.

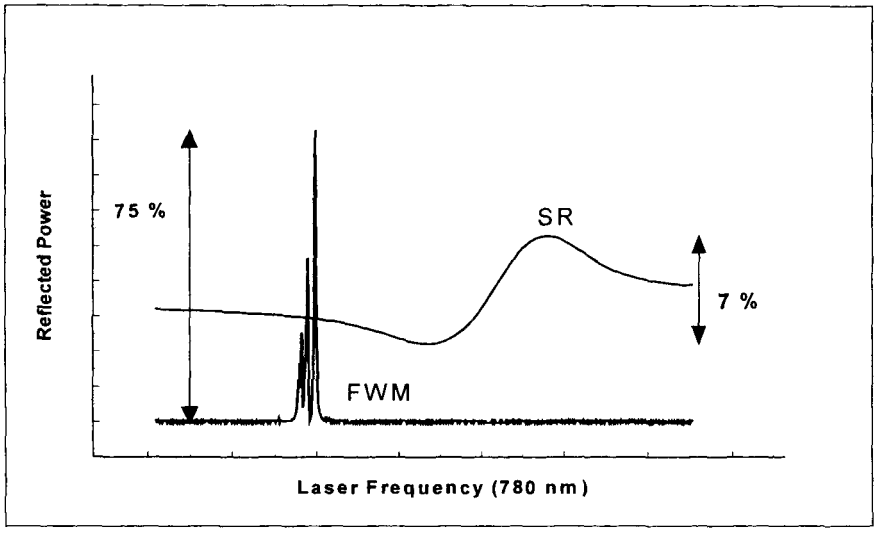

FIGURE 6. Power of the reflected signals detected simultaneously but with two separate photodetectors using the experimental arrangement of fig. 5. The SR signal is the usual Doppler-free selective-reflection signal, and 4WM is the phase-sensitive four-wave-mixing signal. The vertical axis is different for the two curves, but the inset labels show the fraction of power reflected for the individual curves. The 4WM reflection signal even shows gain under some conditions. The horizontal axis is the tuning of the 780 nm probe-laser frequency over a total range of~ 280 MHz. Other experimental parameters are: Power of the 776 nm drive laser = two x 35 mW/ 0.25 nm dia., power of 780 nm probe laser = 0.1 mW/ 0.1 mm dia., with orthogonal polarizations between drive and probe, and T_{cell} = 150 C (423 K).

CASCADE 2-PHOTON DRIVEN FORWARD-4WM "BOX"

The fourth experimental configuration consisted of two co-propagating diode laser beams near resonance with a cascade 2-photon transition in Rb (5S-5P-5D). The goal was to study experimentally the feasibility of making short-wavelength sources of coherent radiation using atomic coherences and diode laser sources. Encouraged by demonstrations of lasing-without-inversion (LWI) in systems that were experimentally convenient, and that had produced lasing at wavelengths near the wavelength of the input coherent-drive, we wanted to push toward shorter wavelengths [17,18].

Of particular interest is the V-configuration, where a strong drive-field can couple the atomic ground state to a low-lying excited state, creating gain on a shorter-wavelength transition between the ground state and a higher-lying energy level. A potential case for demonstrating this concept might be to incoherently populate the Rb 6P state by spontaneous decay from 5D, which can be pumped by a cascade two-photon transition from the ground state (fig. 7.). It should then be possible to apply a

strong coherent-drive between the ground S-state and another level, for example using the D1 transition to the $5P_{1/2}$ (not shown in fig. 7.) to create the desired V-configuration. However, when we started to explore this in the laboratory, even without the coherent-drive on D1, we found that other multi-wave mixing effects became important in the dense Rb vapor.

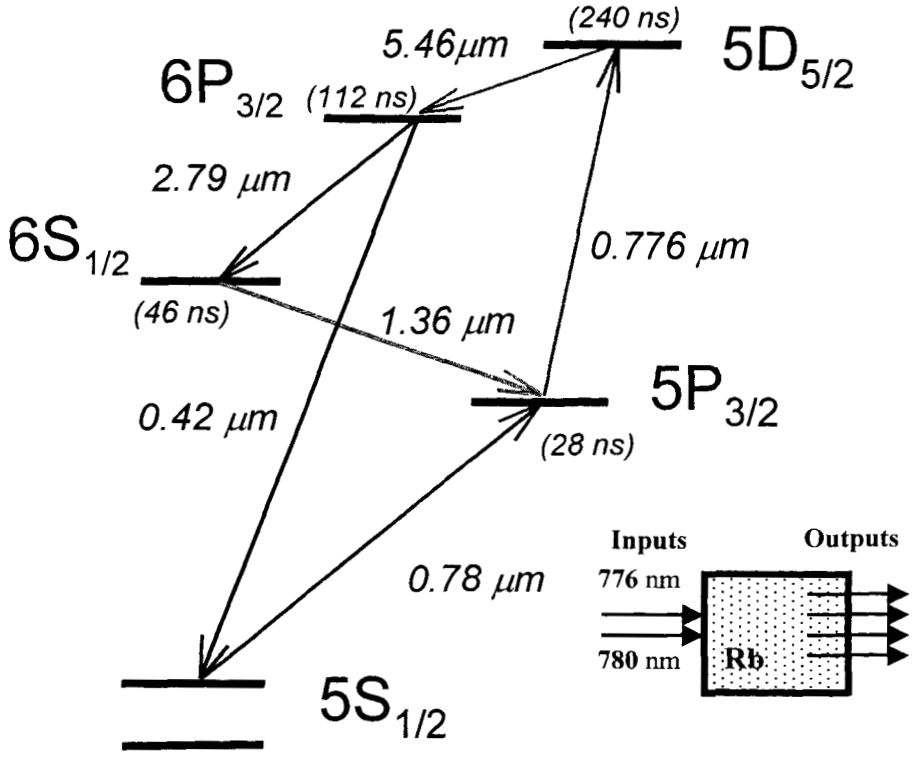

FIGURE 7. Simplified energy-level diagram of Rb showing the two input laser fields at 780 nm and 776 nm, and the coherent output beams at 420 nm, 5.4 μm, 1.36 μm, and ~2.8 μm, that we detected in the forward direction after the Rb cell.

Blue Beam Generation

With the two low-power (780 nm and 776 nm, ≈10 mW each) input laser fields we found that a coherent blue-beam was emitted in the forward direction from the Rb cell, (where "forward" means co-propagating with the two co-propagating input beams). The blue-beam is spectrally narrow, and does, in fact, come from the 420 nm 5S-6P transition. This was achieved even though the vapor cell was optically thick for the 420 nm radiation.

The configuration of two input fields in two-photon cascade (as in fig. 7) may not be an arrangement in which we expect LWI. However, the type of signals that we observe have been detected previously using high-power, short-pulse laser sources, and they have been studied in some detail with those sources [19-22]. This kind of coherent generation is attributed to forward-four-wave-mixing (F-4WM), a nonlinear parametric process. There have also been a number of experimental demonstrations of cw short-wavelength generation using F-4WM by injecting three input laser fields into an atomic vapor to produce a fourth shorter wavelength [23-25]. In a recent impressive experiment, Eikema et al. [26] have used F-4WM to generate ~1 nW of cw, 121 nm light by driving Hg vapor with three input fields. A related 4WM system using 3 input-fields but in a double-Λ configuration, has also been used to produce cw radiation using molecules [27]. Since the F-4WM interaction is quite strong, and apparently easy to initiate, we would not be surprised to learn that these signals had been observed before using just two cw input-fields; however, a preliminary search through the literature did not turn up any such examples.

With our experimental setup we detected as much as 12 microwatts of uni-directional, spectrally narrow, blue output power using two ($\approx$10 mW) laser beams in a single pass through a Rb cell (5 cm long) that was heated to about 95 C (368 K). The 420 nm beam coming out of the cell had a good, round spatial-mode that could be coupled into the TEM_{00} mode of a Fabry-Perot cavity fairly efficiently. We used the Fabry-Perot cavity to estimate the linewidth along with the tuning-rate and -range of the blue-beam. The spectral characteristics of the blue-beam corresponded directly to the spectral characteristics of the sum of the input ECDL lasers: fast linewidth about 200 kHz and low-frequency jitter of a few MHz. The frequency of the blue-light tuned at a rate equal to the tuning of either the 780 nm or 776 nm beam, as would be expected for F-4WM. The continuous tuning-range of the blue light was approximately 200 MHz, limited by our input power levels and the Doppler width of the 5D state. As long as we maintained the 776 nm laser tuning to be near resonance with the cascade two-photon transition (to the 5D state) it was possible to generate the blue-beam for a fairly wide tuning of the 780 nm laser, over a significant fraction of the ground-state hyperfine width (6.8 GHz).

Initially, it seemed surprising that the 420 nm beam could propagate through the Rb vapor cell that was optically thick for the 420 nm radiation. A better understanding of the gain on the blue transition comes from using a separate blue laser to probe the absorbance on the 420 nm, 5S – 6P transition. Figure 8 displays the probe absorption spectrum obtained when the 780 nm and 776 nm lasers are coupled to the two-photon cascade 5S – 5P – 5D. The probe shows a strong, spectrally narrow, gain peak that occurs within the Doppler-broadened absorption line.

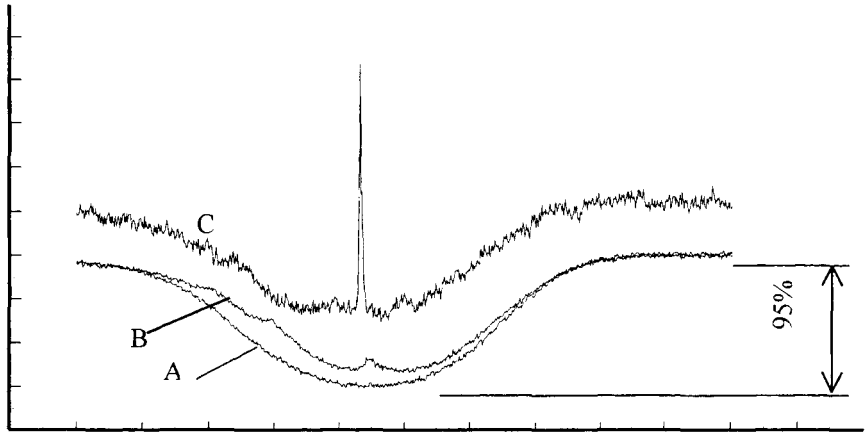

FIGURE 8. An independent, tunable, frequency-doubled diode laser was used to probe the transmission spectrum of the 420 nm (5S – 5D) transition. The vertical axis shows the transmitted power of the probe beam as a function of its tuning over a range of ~500 MHz. Curve A shows the probe transmission with no other laser field present. In curve B the 780 nm laser is also present, and curve C is the probe transmission when both the 780 nm and 776 nm lasers were applied. The sharp peak near the center of the absorption line is the F-4WM gain induced by driving the 780 + 776 nm cascade transition. The increase in the background level and noise that is apparent in curve C results from scattering of the coherent blue light generated by the atoms that also finds its way to the detector. The experimental conditions were: T_{cell} = 95 C, power of 780 nm = 11 mW / 0.5 mm dia., power of 776 nm = 1.8 mW / 0.5 mm dia., and power of 420 nm probe ≈ 30 nW.

The 420 nm probe-beam (power ≈30 nW) was generated by frequency-doubling an ECDL laser in a single-pass through a $LiIO_3$ crystal. This beam was comparatively weak, and did not disturb the character of the blue beam emitted from the Rb cell. It is interesting to note that the Rb atoms are relatively efficient at converting near infrared diode lasers to the shorter blue wavelength. Two 10 mW lasers produced ≈12 microwatts of blue-beam in Rb, whereas similar powers in the nonlinear crystal produced tens of nanowatts. Obviously, nonlinear crystals have numerous advantages (broadly tunable, requires only one input beam, etc.) but the Rb system was simple enough to use, and was more efficient at generating a blue light.

Other Coherent Output Beams

Since the 420 nm blue-beam was strong, and if the interpretation is correct that the source is F-4WM, we expected from the energy-level diagram (fig. 7.) that a 5 μm beam would also be present. Using a new vapor cell constructed from a stainless steel

vacuum tube with commercial sapphire windows we were able to detect a 5 μm beam in the forward direction (fig. 9). There was no evidence of a 5 μm beam in the backward direction. However, it was more difficult to put a stringent upper limit on the lack of a backward beam because, in both cases, the IR detector had a sizable background signal due to the heated Rb cell.

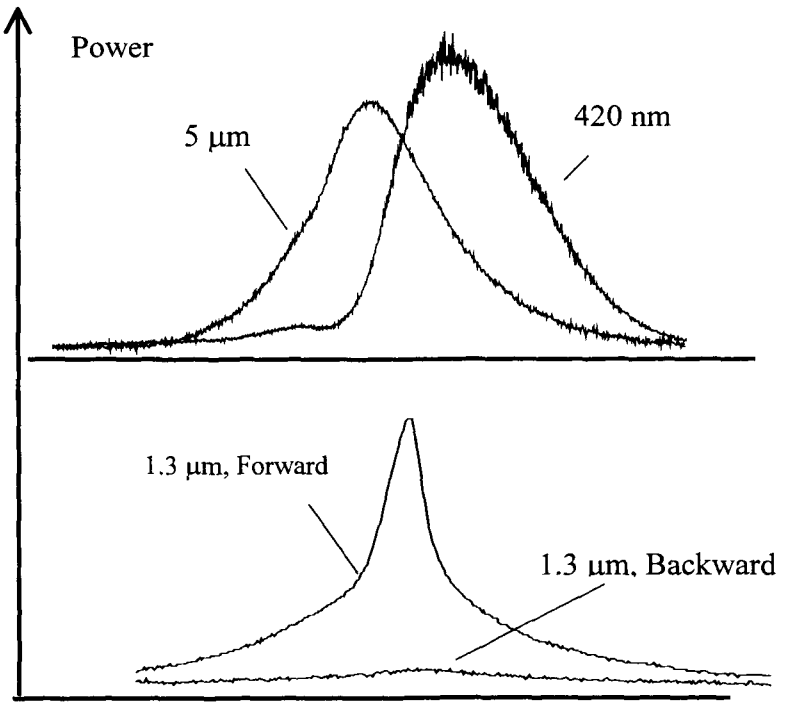

FIGURE 9. The top half of the figure displays the forward powers for the blue beam at 420 nm and the IR beam at 5 μm. These curves were taken simultaneously and are displayed as a function of tuning of the 780 nm laser frequency that was scanned over a total range of ~ 600 MHz. Peak blue power was about 12 microwatts, and the power of the 5 μm was not calibrated. For different tunings of the 776 and 780 nm beams the lower half shows the power in the forward 1.3 μm beam and the lack of a coherent 1.3 μm beam in the backward direction. For this data the experimental parameters were: 780 nm power = 12 mW/0.5 mm dia.; 776 nm = 11 mW/0.5 mm dia.; beams co-propagating with polarizations perpendicular; and T_{cell} = 85 C (358 K).

Additional coherent output beams were generated in the forward direction by adjusting the frequencies of the 780 nm and 776 nm lasers away from the tunings that produced the maximum blue-beam power. These new beams occurred at wavelengths corresponding to other Rb transitions, including: beams at 1.3 μm and ~2.8 μm. Again, we have identified these signals as resulting primarily from F-4WM mixing around closed-loop paths of four energy levels, as indicated in fig.7. The forward 1.3 μm beam was easy to detect, and we used an optical spectrum analyzer to measure its wavelength and thus identify the source as the 6S – 5P transition. The lower half of

fig. 9. shows the unidirectional character of the 1.3 μm signal. A coherent beam was observed in the forward direction, while only spontaneous emission was observed in the backward direction. When the 1.3 μm beam was present, we also detected a forward beam in the wavelength range from 2 to 3.4 μm, which was probably due to the 2.79 μm transition shown in fig. 7. The wavelength discrimination in this case was limited by the responsivity of the InSb detector, combined with a quartz window that served as a long-wavelength cut-off.

With two co-propagating diode laser beams (780 nm and 776 nm) driving the cascade two-photon transition, the Rb atoms provide a very usable coherent blue-beam from a simple heated cell. The processes can be quite efficient, even with low-power cw lasers, and even when one leg of the 4WM box is closed by a spontaneous decay. The dominant process does seem to be F-4WM, but it is likely that additional coherent interactions are playing an important role. In fact, the "box" configuration of 4-levels and 4-photons (two such boxes appear in the Rb energy level diagram in fig. 7.) contains aspects of the well-known 3-level systems. The levels and fields are all coupled coherently and provide a richness of phenomena that depends on the detailed experimental parameters [28-30]. Possibly there are regimes where it would be sensible to regard the "box" configuration as the coherent-coupling of a **V** and a **Λ**, or as a **V** plus a cascade, in analogy with the well known 3-level systems. There may also be conditions where LWI could be found. If the goal is to generate short-wavelength sources, a number of these mechanisms might be used to advantage.

SUMMARY

In all four of the experiments discussed above (the lambda dark-line resonance, the single-beam double-lambda oscillations, and the cascade two-photon transitions in co- and counter-propagating geometries) we observed significant variations from the expected 2-photon coherence lineshapes. These effects were very obvious when the Rb atoms were strongly driven ($\Gamma < \Omega_R < \omega_D$), and when the cells were optically thick. The effects resulted mainly from multilevel, multi-photon coherent interactions that cycle around closed loops in the atomic energy levels. The additional nonlinear terms often dominated the usual 2-photon coherences even at relatively low levels of input power. Though different in outcome and manifestation, these effects can, in some sense, be viewed as multi-wave mixing (predominantly multiple 4-wave mixings) enhanced by the underlying 2-photon coherence.

ACKNOWLEDGMENTS

We thank J. Kitching, N. Vukicevic, S.Harris, T. Mossberg, M. Alegrini, E. Arimondo, R. Wynands, R. Kaiser, P. Hemmer, and M. Fleischhauer for numerous stimulating discussion and comments.

REFERENCES

1. Alzetta, G., Gozzini, A., Moi, L., and Orriols, G., *Nuovo Cimento* **36B**, 5-20 (1976).
2. Arimondo, E., *Progress In Optics* **35**, 257-354 (1996).
3. Fulton, D.J., Shepherd, S., Moseley, R.R., Sinclair, B.D., and Dunn, M.H., *Physical Review A* **52**, 2302-2311 (1995).
4. Vukicevic, N., Zibrov, A.S., Hollberg, L., Walls, F.L., Kitching, J. and Robinson, H.G., IEEE J. FCC (2000).
5. Kitching, J., Knappe, S., Vukicevic, N., Hollberg, L., Wynands, R., and Weidemann, W., proceed. Int. Freq. Cont. Symp. (2000), submitted, IEEE *Trans on Instr. and Meas* (2000).
6. Fleischhauer, M. and Scully, M.O., *Phys. Rev. A,* **49**, 1973 (1994).
7. Wynands, R. and Nagel, A., Appl. Phys. B, **68**, 1-25 (1999).
8. Svanberg, S., Yan, G.-Y., Duffey, T.P., and Schawlow, A.L., *Optics Letters* **11**, 138 (1986).
9. Field, J.E., Hahn, K.H.and Harris, S.E., *Phys. Rev. Lett.*, **67**, 3062-3035 (1999).
10. Harris, S.E., *Physics Today*, 36-42 (July, 1997) and references therein.
11. Grove, T.T., Shahriar, M.S., Hemmer, P.R., Kumar, P., Sudarshanam, V.S., and Cronin-Golomb, M., *Opt. Lett.* **22**, 769-771 (1997). Lü, B., Burkett, W.H., and Xiao, M. *Opt. Letts.* **23**, 804-806, (1998). Köster, E., Kolbe, J., Mitschke, F., Mlynek, J., and Lange, W., *Appl. Phys.* **B**, 201-207 (1984).
12. Fleischhauer, M., Lukin, M.D., Matsko, A.B., and Scully, M.O., *Phys. Rev. Lett.*, **84**, 3558-3561 (2000).
13. Lukin, M.D., Fleischhauer, M., Zibrov, A.S., Robinson, H.G., Velichansky, V.L., Hollberg, L., and Scully, M.O., *Phys. Rev. Lett.* **79**, 2959-2962 (1997). And Zibrov, A.S., Lukin, M..D., and Scully, M.O., *Phys. Rev. Lett.*, **83**, 4049-4052 (1999).
14. Woerdman, J.P., and Schuurmans, *Opt. Commun.*, **14**, 248 (1975).
15. Akulshin, A.M., Velichanskii, V.L., Zibrov, A.S., Nikitin, V.V., Sautenkov, V.A., Yurkin, E.K., and Senkov, N.V., Pis'ma Zh. Eksp. Teor. Fiz. **36**, 247 (1982), [JETP Lett. **36**, 303 (1982)].
16. Amy-Klein, A., Saltiel, S., Rabi, O.A., and Ducloy, M., *Physical Review A* **52**, 3101-3109 (1995). Gorris-Neveux, M., Monnot, P., Saltiel, S., Barbe, R., Keller, J.-C., and Ducloy, M., *Physical Review A* **54**, 3386-3393 (1996).
17. Zibrov, A.S., Lukin, M.D., Nikonov, D.E., Hollberg, L., Scully, M.O., Velichansky, V.L., and Robinson, H.G., *Phys. Rev. Lett.*, 75, 1499-1502 (1995).
18. Scully, M.O., Quantum Opt. 6, 203-215 1994), Mompart, J. and Corbalan, R., *J. Opt. B: Quantum Semiclass* **2**, 1-18 (2000) and references therein.
19. Zhang, P.-L., Wang, Y.-C., and Schawlow, A.L., *J. Opt. Soc. Am. B* **1**, 9-14 (1984).
20. Clark, B.K., Masters, M., and Huennekens, J., *Appl. Phys. B* **47**, 159-167 (1988).
21. Domiaty, U., Gruber, D., Windholz, L., Dinev, S.G., Allegrini, M., De Filippo, G., Fuso, F., Rinkleff, R.-H., *Appl. Phys. B* **59**, 525-531 (1994).
22. Efthimiopoulos, T., Movsessian, M.E., Katharakis, M., and Merlemis, N., *J. Appl. Phys.* **80**, 639-643 (1996).
23. Freeman, R.R., Bjorklund, G.C., Economou, N.P., Liao, P.F., and Bjorkholm, J.E., *Appl. Phys. Lett.* **33**, 739-742 (1978).
24. Wynne, J.J., Sorokin, P.P., Optical mixing in atomic vapors, in Topics in Applied Phys., edt. Shen, Y.R., Springer, Berlin (1987).
25. Nolting, J., Wallenstein, R., *Optics Communications* **79**, 437-442 (1990) and references therein.
26. Eikema, K.S.E, Walz, J., and Hansch, T.W., *Phys. Rev. Lett.* **83** 3828-3831 (1999).
27. Apolonskii, A., Baluschev, S., Hinze, U., Tiemann, E., Wellegehausen, B., *Appl. Phys. B* **64**, 435-442 (1997).
28. Shepherd, S., Fulton, D.J., and Dunn, M.H., *Phys. Rev. A* **54**, 5394-5399 (1996), and references therein.
29. Lvovsky, A.I., and Hartmann, S.R., *Phys. Rev. Lett.* **82**, 4420-4423 (1999).
30. Kosachiov, D.V., Matisov, B.G., and Rozhdestvensky, Y. V., *J. Phys. B: At Mol. Opt. Phys.* **25**, 2473-2488 (1992).